Pressure-induced structural and electronic transitions in FeOOH from first principles

Katrin Otte,[1,*] Rossitza Pentcheva,[1,†] Wolfgang W. Schmahl,[1] and James R. Rustad[2,‡]
[1]*Department of Earth and Environmental Sciences, University of Munich, Theresienstr. 41, 80333 Munich, Germany*
[2]*Geology Department, University of California–Davis, One Shields Avenue, Davis, California 95616, USA*
(Received 23 July 2009; revised manuscript received 23 September 2009; published 18 November 2009)

Using density-functional theory, we investigate the stability, structural, magnetic, and electronic properties of the iron oxyhydroxide polymorphs [α-, β-, γ-, and $hp(\epsilon)$-FeOOH] under hydrostatic pressure. At ambient conditions goethite (α) is the lowest energy phase, consistent with recent calorimetric measurements. Around 6–7 GPa we predict a transformation to the high-pressure $hp(\epsilon)$ phase. This structural transformation is followed by a high-spin to low-spin transition at 7.7 GPa, at much lower pressure than for other currently discussed iron-bearing minerals. While in the ground state the Fe^{3+} ions are coupled antiferromagnetically, at high pressures a strong competition to a ferromagnetic alignment is found in $hp(\epsilon)$-FeOOH. Concerning the electronic properties, including an on-site Coulomb repulsion parameter U (LDA/GGA+U method) improves the size of the zero-pressure band gaps substantially but shifts the spin transition to higher pressure (56.5 GPa). The predicted spin crossover is associated with a blueshift of 0.4 eV.

DOI: 10.1103/PhysRevB.80.205116 PACS number(s): 91.60.Gf, 71.30.+h, 75.30.Wx, 71.27.+a

I. INTRODUCTION

The iron oxyhydroxides (FeOOH) play an important role in nature and technology. They are common minerals in aquifers, sediments, and in the Earth's crust. In the soil they act as natural regulators of concentration and dissolution of nutrients or pollutants such as heavy metals[1,2] and arsenic complexes,[3] thus finding application in the treatment of contaminated water. FeOOH belongs to the group of *X*OOH minerals (*X*=Fe, Al, Mn, Co, and Cr), which crystallize in five canonical oxyhydroxide structures: diaspore, boehmite, akaganeite, guyanaite, and grimaldiite, named after the main representative. The iron oxyhydroxides have been identified crystallographically in the structures of diaspore as goethite (α),[4] of boehmite as lepidocrocite (γ),[5] as akaganeite (β),[6] and of guyanaite as the high-pressure [$hp(\epsilon)$] form.[7]

The FeOOH structures consist of corner-linked bands (single or double) of $FeO_3(OH)_3$ octahedra. The linkage of these bands results in different framework structures as shown in Fig. 1 (see also Table I). In the α phase the double bands of edge-sharing octahedra form 2×1 channels while in β-FeOOH the arrangement of double bands results in 2×2 channels, which are stabilized in nature by a variable amount of molecules such as H_2O and ions such as OH^-, Cl^-, F^-, or NO_3^-. In γ-FeOOH (lepidocrocite), the double bands along the *c* axis form zigzag layers, that are connected to each other via hydrogen bonds (OH$\cdots$O). The iron ions are surrounded by three nonequivalent oxygen atoms as a result of the zigzag sheets. The $hp(\epsilon)$ phase is isostructural to InOOH and the only structure composed of corner sharing single bands of octahedra. This results in a dense 1×1 arrangement along the *c* axis with interstitial hydrogen.

The polymorphs often have high surface areas and high adsorption affinities for aqueous solutes. Therefore, subtle changes in surface chemical environments in terms of temperature, humidity, impurity ions, and crystallization rates can have an important influence on the observed mineral assemblages in low-temperature environments. Their magnetic properties are sensitive to soil redox conditions and solution compositions.[8] Thus, the oxyhydroxide minerals can potentially serve as sensitive recorders of climate history, providing insights into crucial questions concerning the evolution of the Earth's atmosphere on geologic timescales.[9]

Despite the importance of this system in the Earth sciences, there is only one previous theoretical study on the relative stability of the FeOOH polymorphs at zero pressure based on DFT calculations using pseudopotentials.[10] An unexpected finding is that the $hp(\epsilon)$ phase was predicted to be the most stable polymorph at ambient conditions. The discrepancy to recent calorimetric measurements[11,12] has motivated us to revisit this problem employing an all-electron DFT method. Moreover, the high-pressure behavior of hydrous Fe-bearing minerals is important for understanding the processes in the Earth's crust and upper mantle. In this respect FeOOH can be regarded as a model system for achieving a better understanding of the role of hydrogen bonding at high pressures.[13,14] Hence, a main goal of this study is to explore the pressure dependence of the FeOOH polymorphs.

The theoretical description of iron-bearing minerals represents a challenge for first-principles methods due to their complex structure, the localized 3*d* orbitals of Fe, and the influence of correlation effects. Therefore, one aspect of this study is to examine how the level of treatment of electronic correlations influences the energetic, structural, and electronic properties.

In this paper we present a detailed study of the energetic stability of the polymorphs [α-, β-, γ-, and $hp(\epsilon)$-FeOOH] at ambient conditions and under pressure. Moreover, we determine the equation of state and compare the bulk moduli and equilibrium volumes to available experimental data. The focus of the present study lies on pressure-induced structural and spin transitions. We predict that the α phase (goethite) transforms at approximately 6–7 GPa to $hp(\epsilon)$-FeOOH. Furthermore, a collapse from a high-spin (HS) to a low-spin (LS) state is found for the $hp(\epsilon)$ phase. The transition takes place at considerably lower pressures than in magnesiowüstite[15,16] or silicate perovskites,[17,18] which are currently in the center of discussion of spin-crossover phenomena.

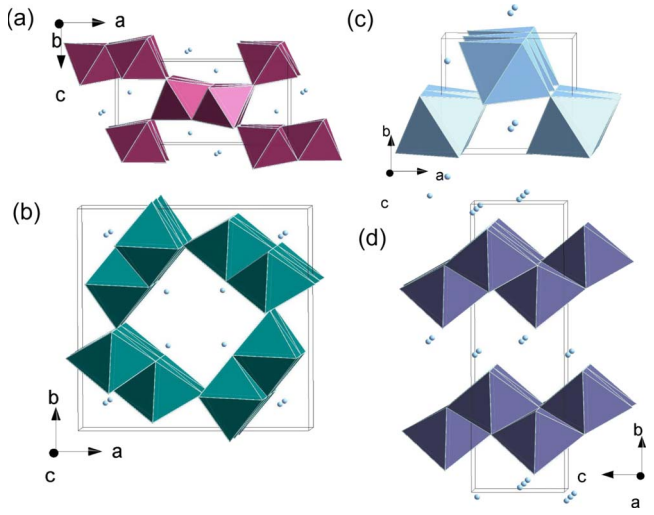

FIG. 1. (Color online) The structures of the FeOOH polymorphs represented in terms of $FeO_3(OH)_3$ octahedra where the hydrogen atoms (in light blue/gray) reside in the 2×1, 2×2, and 1×1 channels of (a) α-FeOOH (goethite), (b) β-FeOOH (akaganeite), and (c) $hp(\epsilon)$-FeOOH, respectively, or between the zigzag sheets of (d) γ-FeOOH (lepidocrocite)

In the following (Sec. II) we discuss briefly the calculational details. In Sec. III we compare the calculated relative energetic stability of the polymorphs to calorimetric measurements.[11] The equation of state of the polymorphs is determined in Sec. IV together with theoretical evidence for a transition from the α- to the $hp(\epsilon)$ phase between 5.9 and 7 GPa. We reexamine previous experimental data and find indications for such a phase transition. In Sec. V we describe the structural changes under pressure. The pressure-induced magnetic and spin transition in $hp(\epsilon)$-FeOOH is discussed in Sec. VI and related to the electronic properties in Sec. VII. The results are summarized in Sec. VIII.

II. CALCULATIONAL DETAILS

The DFT calculations were performed with the full-potential all-electron linear augmented plane-wave method in the WIEN2K implementation.[19] The generalized gradient approximation (GGA) (Ref. 20) of the exchange and correlation potential was used. Because electronic correlations play an important role in transition-metal oxides, we have explored their influence beyond GGA by including an on-site Coulomb repulsion parameter U within the GGA+U approach.[21] While U values obtained from constrained local-density approximation tend to be higher (7–8 eV),[22] a recent study of Fe^{2+} in magnesiowüstite determined U parameters between 5 and 6 eV from linear-response theory.[16] The authors reported also a pressure dependence of the U parameter but the absolute U value changes by less than 1 eV for a volume reduction of 30%. Therefore, in order to compare total energies as a function of pressure, we have used a consistent value of $U=5$ eV and $J=1$ eV on the Fe ions throughout the calculations, similar to other studies on iron oxides.[23,24] Due to the small muffin-tin (MT) radius of hydrogen [$R_{MT}(Fe)=1.9$ bohr, $R_{MT}(O)=1.0$ bohr, and $R_{MT}(H)=0.6$ bohr], a high energy cutoff of 36 Ry was chosen in order to achieve an accuracy of total energies of 1 mRy. For the integration in reciprocal space 48, 21, 84, and 32 $\boldsymbol{k}$ points were used in the irreducible part of the Brillouin zone for the α-, β-, γ-, and $hp(\epsilon)$ phase, respectively. Inside the MTs the wave functions were expanded in spherical harmonics with angular momenta up to $l_{max}^{wf}=10$. Nonspherical contributions to the electron density and potential up to $l_{max}^{pot.}=6$ were used within the MT and a cutoff of 196 Ry in the interstitial.

Information on the structural and magnetic parameters is given in Table I. An optimization of the internal parameters under hydrostatic pressure was performed both within GGA and GGA+U.

III. ENERGETIC STABILITY OF THE FeOOH POLYMORPHS

DFT calculations were carried out for the different polymorphs both for a ferromagnetic (FM) and an antiferromagnetic (AFM) coupling of the Fe ions. For all systems, except for the $hp(\epsilon)$ phase at high pressures, the AFM case is the ground state in agreement with experiment.[25] The energy volume, $E(V)$, as well as the enthalpy pressure, $\Delta H(p)$, relations of the polymorphs are presented in Fig. 2.

TABLE I. Experimental data on the (magnetic) structure of the different polymorphs showing the lattice parameters, volume, space group (SG), Wykoff letter, and multiplicity of the ions (site). The formula units per unit cell ($\frac{\text{f.u.}}{\text{u.c.}}$) correspond to the size of the simulation cell, except for γ-FeOOH, where only 2 f.u. remain in the reduced cell. Additionally, the type of octahedral arrangement and channels in the respective structures is given as well as the Néel temperature and orientation of the spins along the crystallographic axes.

	Lattice parameter								
Phase	a (Å)	b (Å)	c (Å)	V (Å)	SG	Site	$\frac{\text{f.u.}}{\text{u.c.}}$	Octahedra arrangements	T_N spin (K)
Goethite (α)	9.95	3.01	4.62	138.37	*Pnma*	4*c*	4	Double bands, 2×1 tunnels	$400\|\|b$
Akaganeite (β)	10.48	10.48	3.02	332.02	$I\frac{4}{m}$	8*h*	8	Double bands, 1×1 and 2×2 tunnels	$270\|\|c$
Lepidocrocite (γ)	3.07	12.52	3.87	148.91	*Cmcm*	4*a*	4	Zigzag layers	$77\|\|c$
$hp(\epsilon)$ [a]	4.94	4.43	2.99	65.5 1	$Pmn2_1$	2*a*	2	Single bands, 1×1 tunnels	$470\|\|c$

[a]Reference 7.

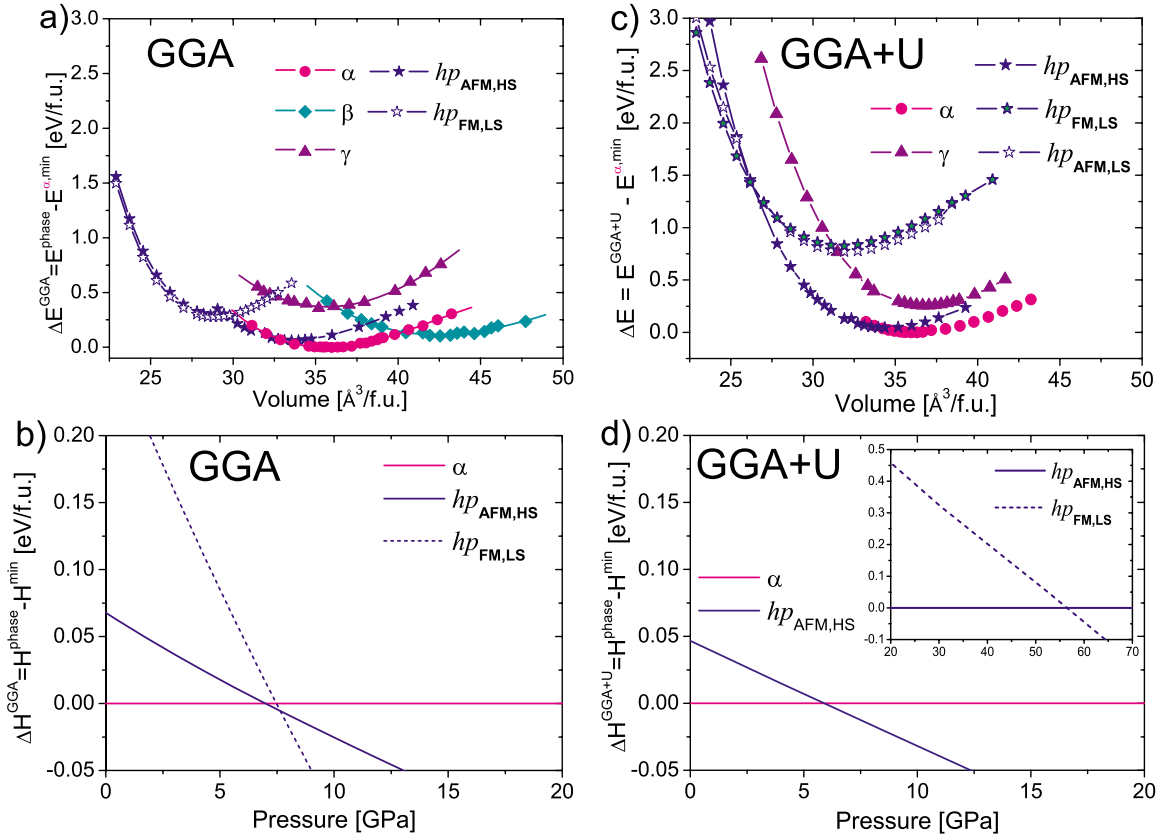

FIG. 2. (Color online) Energy as a function of volume and enthalpy-pressure relation $\Delta H(p)$ for the different polymorphs within GGA (left panels) and GGA+U (right panels). The total energy at the equilibrium volume, V_0, of the most stable α phase is set to zero. $\Delta H(p) < 0$ indicates phases that are more stable than the α-phase [or $hp(\epsilon)_{\mathrm{AFM,HS}}$ in the inset in (d)] for a given pressure.

The relative stabilities of the different phases with respect to the α phase at zero pressure are displayed in Table II. Our results reveal that goethite is the most favorable phase at ambient conditions both within GGA and GGA+U. Within GGA the α phase is followed in stability by the $hp(\epsilon)$ (0.07 eV/f.u.), β- (0.11 eV/f.u.), and γ phase (0.37 eV/f.u.), which is the least stable one. A similar trend is obtained within GGA+U: $hp(\epsilon)$-FeOOH is 0.05 eV/f.u. less favorable than the α phase, followed by the γ phase (0.25 eV/f.u.).

These results agree with calorimetric measurements[11] which found energy differences with respect to the most stable α phase of $\Delta E^{\beta}=0.08$ eV/f.u. and $\Delta E^{\gamma}=0.14$ eV/f.u. [data for the $hp(\epsilon)$ phase were not reported in this study]. These relative stabilities indicate that the framework structure is more favorable than the layered one.

IV. EQUATION OF STATE: EVIDENCE FOR A PHASE TRANSITION

The equation of state is obtained through a third order Birch-Murnaghan (BM) fit.[27] To identify possible phase transitions, we have determined the enthalpy $H=E+pV$, where the pressure is obtained as an energy derivative with respect to the volume $p=-\frac{dE}{dV}$ from the third-order BM fit. In Figs. 2(b) and 2(d) we have plotted the enthalpy difference with respect to the α phase ($\Delta H=H^{phase}-H^{\alpha}$). While goethite is stable at ambient conditions, for negative pressures akaganeite becomes more favorable. At high pressures, our calculations predict that goethite transforms into the $hp(\epsilon)$ phase. The transition pressure is 7 GPa within GGA and slightly lower within GGA+U (5.9 GPa). Furthermore, a spin transition from a high-spin to a low-spin state is found which occurs within GGA at 7.7 GPa and within GGA+U at 56.5 GPa. The respective transition pressures are also listed in Table III.

Table II contains the equilibrium volume V_0, the bulk modulus B_0, and its pressure derivative B_0' for each phase. Experimentally determined volumes are also listed. Bulk moduli are available so far only for the α (Refs. 13 and 26) and the $hp(\epsilon)$ phase.[13] In the following we will discuss the properties of the FeOOH polymorphs and also reexamine previous experimental findings in the context of the predicted phase and spin transitions.

A. Equilibrium volume

Generally, both GGA and GGA+U overestimate the equilibrium volume. For goethite, the GGA/GGA+U values are 2.7%/4.3% larger than the V_0 determined by Szytula *et al.*[4] On the other hand, there is much better agreement to the data reported in a more recent synchrotron x-ray diffraction (XRD) study by Nagai *et al.*[26](1.1%/2.8%). A recent DFT study[28] of goethite obtained similar results (1.1%/5.1% larger than the ones reported by Szytula *et al.*[4]) while the values

TABLE II. Relative stability of the polymorphs ($\Delta E = E^{\text{phase}} - E^{\alpha,\text{min}}$) with respect to the most stable phase (α) calculated within GGA and GGA+U. The results for the equilibrium volume, bulk modulus, and B_0' of the different polymorphs are compared to available experimental data.

Phase	Method	ΔE ($\frac{\text{eV}}{\text{f.u.}}$)	V_0 ($\frac{\text{Å}^3}{\text{f.u.}}$)	B_0 (GPa)	B_0'
α	GGA	0.00	35.5	90.6	5.8
	GGA+U	0.00	36.1	108.8	5.9
	Experiment[a]		34.6		
	Experiment[b] (0–11.0 GPa)			108.5	4
	Experiment[b] (0–24.5 GPa)		35.1	111	4
	Experiment[c] (0–29.4 GPa)		34.7	140.3	4.6
β	GGA	0.11	42.6	76.4	2.1
	GGA+U	0.18	42.6	194.7	1.4
	Experiment[d]		41.5		
γ	GGA	0.37	35.7	107.1	0.7
	GGA+U	0.25	36.8	158.9	4.6
	Experiment[e]		37.0		
AFM coupling					
hp_{HS}	GGA	0.07	33.8	104.0	5.6
	GGA+U	0.05	34.5	123.2	5.7
hp_{LS}	GGA+U	0.76	32.0	152.7	4.6
FM coupling					
hp_{HS}	GGA+U	0.22	34.9	124.3	5.9
hp_{LS}	GGA	0.28	28.9	187.0	6.0
	GGA+U	0.83	31.7	135.1	5.9
hp	Experiment[f]		32.7		
	Experiment[c]		33.2	158	4

[a]Reference 4.
[b]Reference 26.
[c]Reference 13.
[d]Reference 6.
[e]Reference 5.
[f]Reference 7.

obtained by Kubicki *et al.*[29] coincide with the experimental data of Szytula *et al.*[4] both within GGA and GGA+U.

The theoretical equilibrium volume for the $hp(\epsilon)$ phase is 33.8 Å^3 (GGA) and 34.5 Å^3 (GGA+U) again larger than the experimental one (33.15 ± 0.5 Å^3).[13] We find that the predicted pressure-induced spin transition invokes a substantial volume reduction of 14.5%/8.1% within GGA/GGA+U to $V_0^{\text{FM,LS}} = 28.9/31.7$ Å^3.

TABLE III. Respective transition pressures within GGA and GGA+U for the phase transformation from α- to $hp(\epsilon)$-FeOOH as well as the spin crossover in the $hp(\epsilon)$ phase from a HS, AFM to an LS, FM state.

	Phase transition $\alpha \rightarrow hp(\epsilon)$ (GPa)		Spin crossover $hp(\epsilon) \rightarrow hp(\epsilon)$ (GPa)	
Method	HS, AFM	HS, AFM	HS, AFM	LS, FM
GGA	7		7.7	
GGA+U	5.9		56.5	

B. Compressibility

Concerning the bulk moduli, there is an excellent agreement between the GGA+U value for goethite (108.8 GPa) and the experimental bulk modulus determined by Nagai *et al.*[26] in the range 0–11 GPa (108.5 GPa). GGA tends to underestimate the bulk modulus ($B_0^{\text{GGA}} = 90.6$ GPa). Similar values were found by Russell *et al.*[28] We observe a strong dependence of the experimental B_0 on the pressure range used in the fit. For example, Nagai *et al.*[26] obtained 111 GPa using XRD data for 0–24.5 GPa. A substantially higher value of 140.3 ± 3.7 GPa was obtained by Gleason *et al.*[13] who applied a BM fit on XRD data in the pressure range 0–29.4

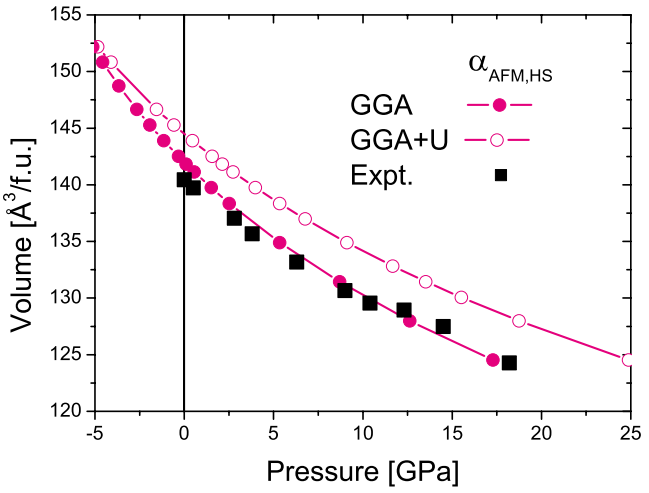

FIG. 3. (Color online) Volume as a function of pressure within GGA (filled circles) and GGA+U (open circles). For comparison, the experimental data of Nagai *et al.* (Ref. 26) (black squares) is added and shows very good agreement with the GGA results.

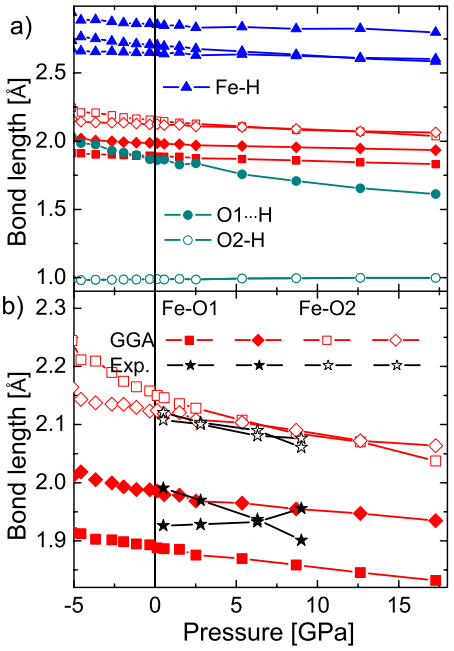

FIG. 4. (Color online) (a) Bond lengths in α-FeOOH as a function of pressure within GGA. (b) Pressure dependence of the Fe-O bonds in α-FeOOH within GGA: the filled symbols denote the different Fe-O1 bonds, the open symbols the different Fe-O2 bonds. Additionally, the bond lengths up to 9 GPa obtained by Nagai *et al.* (Ref. 26) from XRD measurements (black stars).

GPa. This value even exceeds the one for the isostructural diaspore [134.4 ± 1.4 GPa (Ref. 30) and 143.7 GPa (Ref. 31)], that has a substantially smaller volume and is thus expected to have a higher B_0 than goethite. We believe that this variation in the experimental bulk moduli with the pressure interval used in the BM fit is rather related to the phase transformation predicted here from the α- to the $hp(\epsilon)$ phase at 6–7 GPa.

For the $hp(\epsilon)$ phase the bulk moduli are higher than for α-FeOOH: 104 GPa/123 GPa for the HS AFM state within GGA/GGA+U, respectively. The transition to a low-spin state leads to a further increase in B_0. The value determined by Gleason *et al.*[13] (158 ± 5 GPa) is in agreement to the LS state with AFM coupling of the iron spins (152 GPa).

C. Volume-pressure dependence

Further indications for the predicted phase transition can be found in the volume versus pressure dependence presented in Fig. 3. In fact, the $V(p)$ data of Nagai *et al.*,[26] which are also plotted in Fig. 3, exhibit a kink at around 10–11 GPa accompanied by a discontinuous broadening of diffraction peaks. Similar features were observed also by Gleason *et al.*[13] above 8 GPa. Although these features were associated with a solidification of the pressure medium, they may be related to a beginning phase transformation.

V. PRESSURE DEPENDENCE OF THE BOND LENGTHS

In this section we discuss how the bond lengths change under pressure. In goethite there are two different types of oxygen atoms shared between the octahedra: O2 is part of the hydroxyl group in Fe-O2-H while O1 supplies the hydrogen bridge in Fe-O1···H. In Fig. 4(a), the different bond distances in goethite, namely, the Fe-O(1,2), O(1,2)-H, and Fe-H obtained from GGA are plotted as a function of pressure. Bond shortening is observed as a result of compression in all cases but the strongest effect occurs for the hydrogen-bridge distance (O1···H). This indicates that bulk compression takes place through contraction of the channels rather than the FeO_6 octahedra. A similar observation was made in the XRD study of Nagai *et al.*,[26] who found for a 7% volume reduction only 3% contraction of the FeO_6 octahedra.

Due to the different bonds of oxygen to H, there are four distinct Fe-O distances. Their pressure dependence from DFT and experiment is plotted in Fig. 4(b). The bond lengths at 0 GPa range from 1.9 Å (Fe-O1) to 2.15 Å (Fe-O2). We find that the longer Fe-O2 bonds decrease more rapidly than the Fe-O1 bonds with increasing pressure. The DFT-GGA bond lengths are in good agreement with the ones derived from XRD data[26] up to 9 GPa, which are also shown in Fig. 4(b).

OH bond-length variation with pressure

Because H is a weak x-ray scatterer, it is difficult to locate the H atoms from XRD experiments. DFT calculations can provide here useful information on the OH bonds. Fig. 5 presents the variation in the OH bond lengths for the different polymorphs with pressure obtained within GGA. As discussed above, for α-FeOOH the hydrogen bridge shows the strongest variation with pressure while the bond length of the hydroxyl group remains nearly constant (≈1.0 Å). This trend is also observed for the $hp(\epsilon)$ phase, which is the only polymorph, where a symmetrization of O2-H···O1 occurs above 40 GPa. Williams and Guenther[14] measured infrared (IR) spectra of goethite up to 24 GPa and found that a double peak feature at ≈900 cm^{-1} turns into a single peak at 9.8 GPa. Here, the hydrogen reaches a position equidistant to the

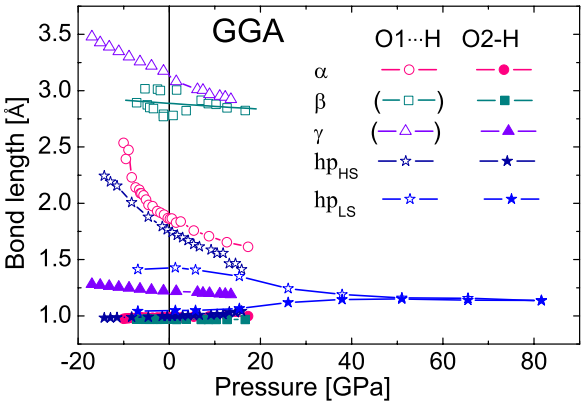

FIG. 5. (Color online) Variation in the hydroxyl bonds (O-H) and the hydroxyl bridges (O···H) for the different phases. The length of the hydrogen-bridge bond exhibits the strongest variation with pressure. In the case of $hp(\epsilon)$-FeOOH, a symmetrization of the OH bonds is observed above 40 GPa.

three Fe ions as in the $hp(\epsilon)$ phase. This feature may be related to the predicted phase transition.

In akaganeite, the oxygen-hydrogen distances remain nearly constant with pressure. This is also true for the O-H bond length in the layered γ-FeOOH of $\approx$1.2 Å, somewhat longer than the typical length in a hydroxyl group. On the other hand, the O···H bridge is reduced from 3.1 Å at ambient conditions to 2.9 Å at 15 GPa.

VI. MAGNETIC PROPERTIES AND PRESSURE-INDUCED SPIN CROSSOVER

The orientation of the spins with respect to the crystallographic axes are specified in Table I (last column). As mentioned previously, we have investigated both ferromagnetic and antiferromagnetic coupling of the Fe ions. For the latter case we have adopted the experimentally suggested magnetic structure.[25] This magnetic order is determined by two main interactions (following the scheme of Coey[32]): (i) a strong AFM coupling of Fe in corner sharing octahedra with an Fe-O-Fe bond angle close to 120° and (ii) a weak AFM coupling for edge-sharing octahedra (i.e., within the double bands) with a Fe-O-Fe bond angles close to 90°.

Table IV shows the magnetic moments of Fe ions in the different phases as well as the energy difference between the FM and AFM coupling ($\Delta E = E_{\mathrm{FM}} - E_{\mathrm{AFM}}$) at the experimental volume. At zero pressure the AFM order is clearly the ground state for all phases ($\Delta E > 0$), in agreement with experimental observations.[25] A stronger competition between the AFM and FM coupling is found only for lepidocrocite: $\Delta E_{\gamma} = 0.07$ eV compared to $\Delta E_{\alpha} = 0.42$ eV. This finding is consistent with the much lower Néel temperature for the γ phase ($T_{\mathrm{N}} = 77$ K) than for the α phase ($T_{\mathrm{N}} = 400$ K).

For all phases except for γ-FeOOH we observe a HS-LS transition in the FM case within GGA. We find that in the AFM state the magnetic moments at V_{exp} are higher (3.61 μ_B) than in the FM state (3.39 μ_B) and remain in a HS configuration under pressure with only a small reduction. The magnetic moments within GGA+U (4.14 μ_B) are larger compared to GGA. This is related to a reduced occupation in the minority-spin channel, as will be discussed in the next section. For goethite iron remains in HS state within the studied pressure range.

On the other hand, in the $hp(\epsilon)$ phase there is a transition from AFM coupled Fe ions in high-spin state to a FM coupling with a low-spin configuration and a magnetic moment of 0.97 μ_B. Within GGA the spin transition takes place at 7.7 GPa [see Fig. 2(b) dashed line] while within GGA+U

TABLE IV. Magnetic and electronic properties of the polymorphs. ΔE denotes the energy difference between the FM and AFM order in GGA ($\Delta E = E_{\mathrm{FM}} - E_{\mathrm{AFM}}$). Additionally, the magnetic moments as well as the calculated and experimental band gaps (Ref. 25) of all phases within GGA and GGA+U are displayed both for the experimental volume and the respective minimum volume, i.e., at maximum pressure. (m=metallic).

		ΔE ($\frac{\mathrm{eV}}{\mathrm{f.u.}}$)	Magnetic moments, M (μ_B)				Band gaps, Δ_g^{phase} (eV)				
		@V_{exp}	@V_{exp}		@V_{min}		@V_{exp}		@V_{min}		Expt. (Ref. 25)
		GGA	GGA	GGA+U	GGA	GGA+U	GGA	GGA+U	GGA	GGA+U	@p=0
α	FM	0.42	3.39	4.21	0.85	0.95	m	1.47	m	2.84	
	AFM		3.61	4.13	3.41	4.10	0.27	2.21	0.15	2.04	2.10
β	FM	0.55	2.87	4.21	0.86	0.96	m	1.43	m	1.79	
	AFM		3.58	4.12	3.21	4.05	0.57	2.44	0.12	1.43	2.12
γ	FM	0.07	3.72	4.21	3.20	3.24	m	1.61	m	m	
	AFM		3.85	4.18	2.79	4.01	m	1.69	m	m	2.06
hp_{HS}	FM			4.22		4.18		1.6		0.24	
	AFM		3.57	4.13		3.88	0.28	2.07		1.00	1.94
hp_{LS}	FM	0.21	0.88/0.84	0.99	0.86	0.93	m	2.40	m	2.46	
	AFM			1.02/0.96	0.84	0.93/0.90		1.90	m	1.30	

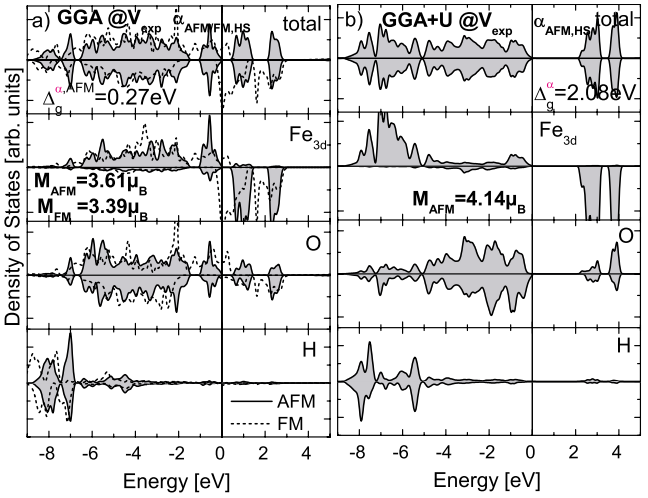

FIG. 6. (Color online) DOS of α-FeOOH at V_{exp}. The left panel shows the GGA results for the FM (dashed line) and AFM coupling (solid line, gray area), the right one the GGA+U results for AFM. V_{exp} corresponds to pressures of 2 GPa within GGA and 4 GPa within GGA+U, respectively.

the HS state collapses to the LS state at a much higher pressure of 56.5 GPa [inset in Fig. 2(d) dashed line]. The $E(V)$ relation within GGA+U [Fig. 2(c)] reveals for Fe in the low-spin state a strong competition between the ferromagnetic and the antiferromagnetic coupling in $hp(\epsilon)$-FeOOH.

We note that no intermediate spin states were obtained in FeOOH. Such have recently been reported for ferrous iron (Fe^{2+}) in lower mantle (post)perovskites.[33,34]

VII. ELECTRONIC PROPERTIES

A. Band gaps

The density of states (DOS) of the different phases were calculated at the experimental volume as well as under pressure. The DOS of the most stable polymorph goethite at the experimental volume within GGA [Fig. 6(a)] shows the sensitive influence of the magnetic coupling on the electronic properties: for FM order the system is metallic while the AFM ground state shows insulating character. However, GGA ($\Delta_g^{\alpha,\mathrm{GGA}}$=0.27 eV) substantially underestimates the experimental band gap of 2.1–2.5 eV.[25,35] Including correlation effects within GGA+U [see Fig. 6(b)] improves the size of the band gap to $\Delta_g^{\alpha,\mathrm{GGA}+U}$=2.08 eV in close agreement with the experimental value. Additionally, the type of band-gap changes from a Mott-Hubbard type (GGA) between empty and occupied Fe 3d states to a charge-transfer type (GGA+U), separating the occupied O 2p from unoccupied Fe 3d states. Analogous behavior was obtained for α-Fe_2O_3.[24,36]

The electronic properties of the other polymorphs given in Table IV show similar trends. While all FM coupled phases are metallic within GGA (except for β), the AFM coupled systems have nonzero band gaps (except for lepidocrocite), which are strongly underestimated compared to experiment. At high pressures, the small band gaps are further reduced to a pseudogap (α and β) or the system becomes metallic

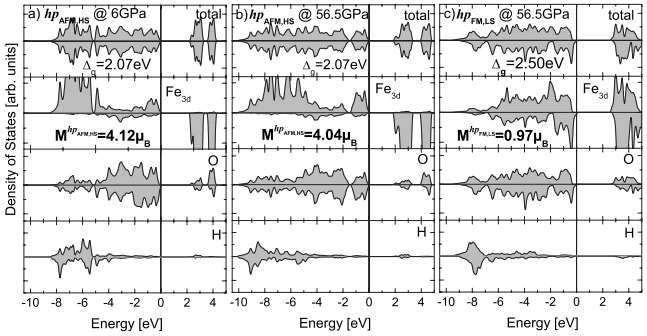

FIG. 7. DOS of $hp(\epsilon)$-FeOOH illustrating the spin transition associated with a change in magnetic order obtained within GGA+U: (a) $hp(\epsilon)$-FeOOH (AFM, HS) at the phase transition pressure of 5.9 GPa; at 56.5 GPa the spin crossover takes place in $hp(\epsilon)$-FeOOH from (b) an AFM, HS state to (c) an FM, LS state.

[$hp(\epsilon)$] within GGA. GGA+U reduces the hybridization between Fe 3d and O 2p bands and leads to a charge-transfer type of band gap with band widths in close agreement to the experimental values.

B. Pressure-induced spin transition in $hp(\epsilon)$-FeOOH

The DOS of $hp(\epsilon)$-FeOOH with antiferromagnetically coupled Fe in high-spin state obtained within GGA+U at the respective phase and spin transition pressures of 5.9 and 56.5 GPa is presented in Figs. 7(a) and 7(b). At 56.5 GPa the valence band is approximately 1.5 eV broader than at 6 GPa. Additionally, the hybridization between Fe 3d and O 2p states is substantially increased. For the HS state all Fe 3d orbitals in the majority-spin channel are occupied, the ones in the minority-spin channel are empty. A substantial rearrangement takes place with the spin transition [Fig. 7(c)]: two electrons now occupy t_{2g} states in the minority-spin channel while the e_g orbitals are empty for both spin directions. As a result, the lower Hubbard band is narrowed by approximately 1 eV and there is a blueshift of the band gap from 2.07 eV (AFM, HS) to 2.50 eV (FM, LS) at 56.5 GPa. A similar effect was reported, e.g., in $(Mg,Fe)SiO_3$.[18] The change in orbital occupation is visualized also in Fig. 8 which shows the spin-density distributions of Fe^{3+} at the spin transition pressure (GGA+U). While in the HS state [Fig. 8(a)] all Fe 3d orbitals are singly occupied leading to a spherical spin-density distribution, the LS state [Fig. 8(b)]

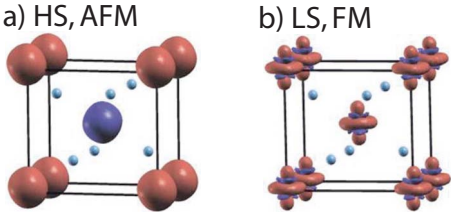

FIG. 8. (Color online) Spin-density distribution of $hp(\epsilon)$-FeOOH at 56.5 GPa for Fe^{3+} in (a) HS, AFM and (b) LS, FM state. Fe is octahedrally coordinated by oxygen (light blue/gray); the hydrogen positions are not shown.

exhibits a clear t_{2g} character with lobes pointing to the faces of the surrounding oxygen octahedron.

VIII. SUMMARY

In summary, we present a comprehensive DFT study of the bulk properties of the FeOOH polymorphs goethite (α), akaganeite (β), lepidocrocite (γ), and the $hp(\epsilon)$ phase at ambient conditions and under hydrostatic pressure. We find that at zero-pressure goethite is the lowest energy phase. Akaganeite becomes favorable only upon volume expansion, which suggests that it is stabilized at ambient conditions by additional ions in its channels. At ambient conditions the α phase is followed in stability by the $hp(\epsilon)$-, β-, and γ phases. The energetic relations among the phases show that the framework structures [α, $hp(\epsilon)$, and β] are more favorable than the layered one (γ) and are in agreement with the trends obtained from calorimetric measurements of Laberty and Navrotsky.[11] Thus, overall, the observed occurrences of these phases in the field are consistent with the calculated cohesive energies and do not appear to be governed primarily by kinetics or surface effects.

A pressure-induced transition from the α- to the $hp(\epsilon)$ phase is predicted at 6–7 GPa. This finding is supported by previous IR data by Ref. 14. Furthermore, Ref. 37 reported the synthesis the $hp(\epsilon)$-phase samples at pressures of 8 GPa, similar to the predicted transition pressure. Voigt and Will[38] determined the boundary line between α- and $hp(\epsilon)$-FeOOH in the range between 6 and 7.5 GPa at temperatures above 573 K. This is confirmed by recent XRD measurements[13] pointing also at a slow conversion from α- to $hp(\epsilon)$-FeOOH above 5 GPa and below 573 K. Further studies will be necessary to shed more light on this transition.

Furthermore, the structure influences not only the stability but also the compressibility. Due to its large 2×2 channels, akaganeite is most compressible. For goethite the bulk modulus obtained within GGA+U (108.8 GPa) is in very good agreement with the value obtained from XRD experiments (108.5 GPa).[26] The bulk modulus of the $hp(\epsilon)$ phase is significantly higher (152.7 GPa for HS AFM), again in good agreement with very recent experimental data (158 GPa).[13] We are not aware of any previous results in the literature for the other FeOOH phases.

The pressure dependence of the bond lengths for the α phase is in good agreement with experiment.[26] The O$\cdots$H bridge of the α- and $hp(\epsilon)$ phase shows the strongest change with pressure indicating that compression takes place by contracting the channels. For the $hp(\epsilon)$ phase a symmetrization of the O-H bonds occurs beyond 40 GPa.

While GGA shows a closer agreement to experiment concerning the equilibrium volume as well as the pressure dependence of the volume and bond lengths, GGA+U provides a better description of the bulk moduli and improves considerably the band gaps. Under ambient conditions all phases are coupled antiferromagnetically and insulating. For the $hp(\epsilon)$ phase we find a HS-LS transition at 7.7 GPa within GGA. Because GGA+U tends to stabilize the HS state, this transition is shifted to 56.5 GPa. Still these pressures are significantly lower than the values reported, e.g., for iron-bearing perovskites or magnesiowüstite and may suggest that the presence of OH^- in the coordination shell of Fe^{3+} facilitates the HS-LS transition. One possible explanation may be the symmetry breaking caused by having both OH^- and O^{2-} in the coordination polyhedron. If this is a general phenomenon, it may indicate an unanticipated connection between water content and the spin-transition pressure in the Earth's mantle. We hope that the results presented here will inspire new experiments to explore the phase transition and possible spin crossover in FeOOH and to determine the bulk moduli of the FeOOH polymorphs.

ACKNOWLEDGMENTS

We acknowledge support through DOE under Grant No. DE-FG02-04ER15498. Simulations are performed on the high-performance supercomputer at the Leibniz Rechenzentrum.

*katrin.otte@lrz.uni-muenchen.de
†pentcheva@lrz.uni-muenchen.de
‡rustad@geology.ucdavis.edu

[1] B. A. Manning, J. R. Kiser, H. Kwon, and S. R. Kanel, Environ. Sci. Technol. **41**, 586 (2007).
[2] U. Schwertmann, NATO ASI Ser., Ser. B **217**, 267 (1988).
[3] M. Stachowicz, T. Hiemstra, and W. H. van Riemsdijk, J. Colloid. Interface Sci **302**, 62 (2006).
[4] A. Szytula, A. Burewicz, Z. Dimitrijevic, S. Krasnicki, H. Rzany, and J. Todorovic, Phys. Status Solidi **26**, 429 (1968).
[5] H. Christensen and A. N. Christensen, Acta Chem. Scand. **32a**, 87 (1978).
[6] A. L. MacKay, Mineral. Mag. J. Mineral. Soc. **32**, 545 (1960).
[7] M. Pernet, J. C. Joubert, and C. Berthet-Colominas, Solid State Commun. **17**, 1505 (1975).
[8] F. LaGroix and S. K. Banerjee, Earth Planet. Sci. Lett. **225**, 379 (2004).
[9] C. J. Yapp, Annu. Rev. Earth Planet Sci. **29**, 165 (2001).
[10] K. M. Rosso and J. R. Rustad, Am. Mineral. **86**, 312 (2001).
[11] C. Laberty and A. Navrotsky, Geochim. Cosmochim. Acta **62**, 2905 (1998).
[12] A. Navrotsky, L. Mazeina, and J. Majzlan, Science **319**, 1635 (2008).
[13] A. E. Gleason, R. Jeanloz, and M. Kunz, Am. Mineral. **93**, 1882 (2008).
[14] Q. Williams and L. Guenther, Solid State Commun. **100**, 105 (1996).
[15] J. Badro, J.-P. Rueff, G. Vanko, G. Monaco, G. Fiquet, and F. Guyot, Science **305**, 383 (2004).
[16] T. Tsuchiya, R. M. Wentzcovitch, C. R. S. da Silva, and S. de Gironcoli, Phys. Rev. Lett. **96**, 198501 (2006).
[17] S. Stackhouse, J. P. Brodholt, and G. D. Price, Earth Planet. Sci.

Lett. **253**, 282 (2007).
[18] K. Umemoto, R. M. Wentzkowitch, Y. G. Yu, and R. Requist, Earth Planet. Sci. Lett. **276**, 198 (2008).
[19] P. Blaha, K. Schwarz, G. K. H. Madsen, D. Kvasnicka, and J. Luitz, *wien2k, An Augmented Plane Wave plus Local Orbitals Program for Calculating Crystal Properties* (Karlheinz Schwarz, Technical University of Wien, Austria, 2001).
[20] J. P. Perdew, K. Burke, and M. Ernzerhof, Phys. Rev. Lett. **77**, 3865 (1996).
[21] V. I. Anisimov, I. V. Solovyev, M. A. Korotin, M. T. Czyzyk, and G. A. Sawatzky, Phys. Rev. B **48**, 16929 (1993).
[22] G. K. H. Madsen and P. Novak, Europhys. Lett. **69**, 777 (2005).
[23] I. Leonov, A. N. Yaresko, V. N. Antonov, M. A. Korotin, and V. I. Anisimov, Phys. Rev. Lett. **93**, 146404 (2004).
[24] G. Rollmann, A. Rohrbach, P. Entel, and J. Hafner, Phys. Rev. B **69**, 165107 (2004).
[25] R. M. Cornell and U. Schwertmann, *The Iron Oxides* (Wiley, Weinheim, 2001).
[26] T. Nagai, H. Kagi, and T. Yamanaka, Am. Mineral. **88**, 1423 (2003).
[27] F. D. Murnaghan, Proc. Natl. Acad. Sci. U.S.A. **30**, 244 (1944).
[28] B. Russell, M. Payne, and L. C. Ciacchi, Phys. Rev. B **79**, 165101 (2009).
[29] J. D. Kubicki, K. W. Paul, and D. L. Sparks, Geochem. Trans. **9**, 4 (2008).
[30] K.-D. Grevel, M. Burchard, D. W. Fasshauer, and T. Peun, J. Geophys. Res., [Solid Earth] **105**, 27877 (2000).
[31] A. Friedrich, D. J. Wilson, E. Haussühl, B. Winkler, W. Morgenroth, K. Refson, and V. Milmann, Phys. Chem. Miner. **34**, 145 (2007).
[32] J. M. D. Coey, in *Iron in Soils and Clay Minerals*, edited by J. W. Stucki, B. A. Goodman, and U. Schwertmann (D. Reidel, Dordrecht, 1988), p. 397–466.
[33] J.-F. Lin, H. Watson, G. Vankó, E. E. Alp, V. B. Prakapenka, P. Dera, V. V. Struzhkin, V. V. Kubo, J. Zhao, C. McCammon, and J. Evans, Nature Geoscience **1**, 688 (2008).
[34] C. McCammon, I. Kantor, O. Narygina, J. Rouquette, U. Ponkratz, I. Sergueev, M. Mezouar, V. Prakapenka, and L. Dubrovinsky, Nature Geoscience **1**, 684 (2008).
[35] D. M. Sherman, Geochim. Cosmochim. Acta **69**, 3249 (2005).
[36] J. Velev, A. Bandyopadhyay, W. H. Butler, and S. K. Sarker, Phys. Rev. B **71**, 205208 (2005).
[37] M. Pernet, J. Chenavas, and J. C. Joubert, Solid State Commun. **13**, 1147 (1973).
[38] R. Voigt and G. Will, Neues Jahrb. Mineral. Abh. **2**, 89 (1981).